Journal of Global Engineering Research & Science (J-GERS)
Vol. 04, No. 02, December 2025, pp. 76-82
ISSN: 2830-5906, *e*-ISSN: 2830-5418, DOI: 10.56904/j-gers.v4i2.161

The Influence of Substrate Width Ratio on the Rectified DC Output Voltage of a Piezoelectric Energy Harvester

Agung Dwi Santoso[1], Adhes Gamayel[1*], Untung Suprihadi[2]
[1] Department of Mechanical Engineering, Faculty of Engineering & Computer Science, Jakarta Global University, Indonesia, 16412
[2] Department of Informatics Engineering, Faculty of Engineering & Computer Science, Jakarta Global University, Indonesia, 16412

Article Info

Article history:

Received September 03, 2025
Revised November 01, 2025
Accepted November 26, 2025

Keywords:

Piezoelectric Energy Harvester
Wind energy harvesting
Micro windmill
Output voltage
Wind tunnel experiment

ABSTRACT

Piezoelectric energy harvesters (PEHs) have attracted considerable attention as an alternative approach for converting ambient mechanical energy into electrical power, particularly under low-speed wind conditions. In this study, the performance of a micro-windmill-driven piezoelectric wind energy harvesting system is experimentally investigated with emphasis on the effects of wind speed and substrate-to-blade width ratios. Experiments were conducted in a controlled wind tunnel environment at wind speeds of 6, 7, and 8 m/s to represent low to moderate airflow conditions commonly encountered in practical applications. Three substrate-to-blade width ratios, namely 1:3, 1:2, and 1:1, were evaluated to assess their influence on the dynamic response and electrical output of the piezoelectric element. The alternating voltage generated by the piezoelectric harvester was rectified, and the output voltage–time characteristics were recorded over a 60 s testing period using a data acquisition system. The experimental results demonstrate that increasing wind speed significantly improves both the voltage rise rate and the achievable steady-state voltage for all tested configurations, indicating enhanced mechanical excitation and energy conversion efficiency at higher airflow velocities. Among the configurations examined, the 1:1 ratio consistently exhibits the highest output voltage and the fastest response, particularly at wind speeds of 7 and 8 m/s, suggesting an optimal mechanical–electrical coupling. The 1:2 configurations show comparable performance at lower wind speeds, while the 1:3 configuration produces substantially lower voltage output throughout the test duration, reflecting reduced energy transfer effectiveness. Overall, the findings highlight the importance of mechanical configuration and wind speed in determining the performance of piezoelectric wind energy harvesters. The results provide useful design guidelines for optimizing PEH systems intended for self-powered sensors and other low-power electronic applications operating in low-speed wind environments.

Corresponding Author:

Adhes Gamayel
Department of Mechanical Engineering, Faculty of Engineering & Computer Science, Jakarta Global University, Indonesia, 16412
Email: adhes@jgu.ac.id

1. INTRODUCTION

Energy harvesting has emerged as a promising solution to power distributed and low-power electronic systems by converting ambient energy sources such as mechanical vibrations, wind, acoustic waves, and physiological motion, into usable electrical energy. This approach is particularly important for autonomous sensors, wireless monitoring systems, Internet of Things (IoT) devices, and implantable biomedical electronics, where conventional batteries suffer from limited lifetime and maintenance challenges [1], [2]. Among various transduction mechanisms, including electromagnetic, electrostatic, and thermoelectric methods, piezoelectric energy harvesting has attracted significant attention due to its high energy density, scalability across length scales, and ability to directly convert mechanical strain into electrical charge. Owing to these advantages,

piezoelectric energy harvesters are widely explored for applications ranging from structural health monitoring and noise attenuation to biomedical implants and low-frequency wind energy conversion [3], [4], [5].

Recent studies on piezoelectric energy harvesting have focused on improving power output, operational bandwidth, mechanical durability, and material performance through advanced structural design, material optimization, and Multiphysics modelling. Mechanical stiffness matching between the host structure and piezoelectric material has been demonstrated as an effective strategy to enhance energy transfer efficiency, achieved through tailored beam stiffness and engineered piezocomposites [6]. At the material level, parametric estimation methods have enabled accurate determination and optimization of piezoelectric properties in single crystals, improving reliability and reducing experimental complexity [7], while size-dependent behaviors in piezoelectric nanostructures have been systematically reviewed using modified continuum theories [2]. Structural optimization studies have shown that non-uniform geometries, bistable and monostable configurations, and wave-inspired or galloping mechanisms can significantly enhance output power at low excitation frequencies and low wind speeds [8], [9], [10]. Furthermore, analytical and numerical investigations of piezoelectric-integrated smart structures, including viscoelastic functionally graded plates, micropumps, and sandwich panels, have expanded the applicability of PEH in adaptive structures, fluidic systems, and noise control [5], [11], [12]. Experimental studies under static and dynamic loading conditions have also highlighted the strain-rate-dependent electromechanical response and durability limits of commonly used piezoceramics such as PZT5H, emphasizing the need for improved material design and configuration [13], [14]. Collectively, these advancements underscore the rapid evolution of piezoelectric energy harvesting toward more efficient, robust, and application-specific energy solutions.

Building upon our previous experimental investigations into piezoelectric energy harvesting driven by wind-induced mechanical excitations, this study aims to further elucidate the role of windmill blade configuration in optimizing energy harvesting performance. Earlier works demonstrated that direct collision mechanisms between rotating elements and piezoelectric cantilevers significantly enhance voltage output, with ceramic materials outperforming PVDF due to their higher piezoelectric coefficients, stronger polarization, and greater mechanical rigidity, while flexible plastic fins provided superior impact stability [15]. Subsequent studies revealed that geometric parameters such as substrate-to-mass ratio strongly influence cantilever deflection and voltage generation, where larger mass and cross-sectional ratios promoted increased curvature and collision frequency, leading to higher output voltage [16]. In parallel, vortex-induced vibration (VIV) mechanisms were shown to generate sustained oscillations, with rhombus bluff bodies producing stronger wake-induced pressure fluctuations and improved voltage output compared to square and triangular configurations [17]. A comprehensive review of these excitation strategies, including direct collision, rotational-based collision, and vortex-induced vibration (VIV), highlighted that efficient energy harvesting is governed by the interaction between aerodynamic forces, impact dynamics, and piezoelectric material response [18]. This research aims to investigate the fundamental relationship between the structural geometry of a piezoelectric transducer and its electrical performance under direct excitation. Specifically, the objective is to analyze how variations in the substrate width ratio influence the rectified DC output voltage generated through a direct collision mechanism. By focusing on the interplay between mechanical impact dynamics and AC-to-DC power conditioning, this study seeks to identify the optimal substrate dimensions required to maximize energy conversion efficiency. The resulting data will provide a precise framework for designing high-performance piezoelectric harvesters capable of delivering stable DC power for low-power electronic applications.

2. METHOD

The experimental configuration employed in this study follows the setup described in previous research [16]. The Piezoelectric Energy Harvester (PEH) designed for this study utilizes a piezoelectric bimorph bonded to a rectangular polypropylene substrate. Bimorph configurations are frequently preferred in energy harvesting research as they incorporate an additional active layer without imposing significant design constraints [19]. Lead Zirconate Titanate (PZT) was selected as the active material due to its superior piezoelectric coefficients, high electromechanical coupling, and high dielectric constants [20]. Compared to other piezoelectric materials, PZT exhibits greater tolerance for stress and strain, which directly correlates to increased power generation [21]. The specific PZT dimensions employed are 8 cm in length, 3 cm in width, and 0.6 mm in thickness. This bimorph is mounted onto a flexible polypropylene substrate (10 cm × 6 cm × 1 mm), chosen for its excellent anti-fatigue properties. To facilitate energy conversion through mechanical excitation, an impact area of 5 mm was established between the PEH and the striking blade. The experimental setup focuses on the deflection-induced voltage generated by these collisions, specifically evaluating the performance across three distinct substrate-to-blade width ratios: 1:1, 1:2, and 1:3. The detailed specifications of the PZT material are presented in Table 1, while the various substrate width ratios utilized in the experimental setup are illustrated in Figure 1. The ratio is defined as the width of the substrate relative to that of the micro windmill blade.

e-ISSN: 2830-5418, *p*-ISSN: 2830-5906

Table 1. Specification of PZT

No.	Properties	Values
1	Density (x10^3 kg/m3)	7500
2	Young modulus (GPa)	56
3	Poisson's Ratio	0.36
4	Piezoelectric Strain Coefficient (d_{31}) C/N	-186 x 10^{-12}
5	Permittivity at constant stress ($\varepsilon_{11}{}^{T}/\varepsilon_0$)	3130
6	Permittivity at constant strain ($\varepsilon_{33}{}^{S}/\varepsilon_0$)	3400

Table 1 summarizes the key material properties of Lead Zirconate Titanate (PZT), a commonly used piezoelectric ceramic. The density of 7500 kg/m³ indicates a relatively heavy ceramic material, while the Young's modulus of 56 GPa reflects its high stiffness and ability to withstand mechanical stress. Poisson's ratio of 0.36 describes the material's lateral deformation under loading. The piezoelectric strain coefficient d_{31} of -186×10^{-12} C/N indicates strong electromechanical coupling, enabling efficient conversion between mechanical and electrical energy. The high relative permittivity values at constant stress (3130) and constant strain (3400) demonstrate the material's excellent dielectric behavior, making PZT suitable for applications such as sensors, actuators, and energy harvesting devices.

(a) (b) (c)

Figure 1. Schematic representation of the substrate-to-blade width ratios: (a) 1:1, (b) 1:2, and (c) 1:3

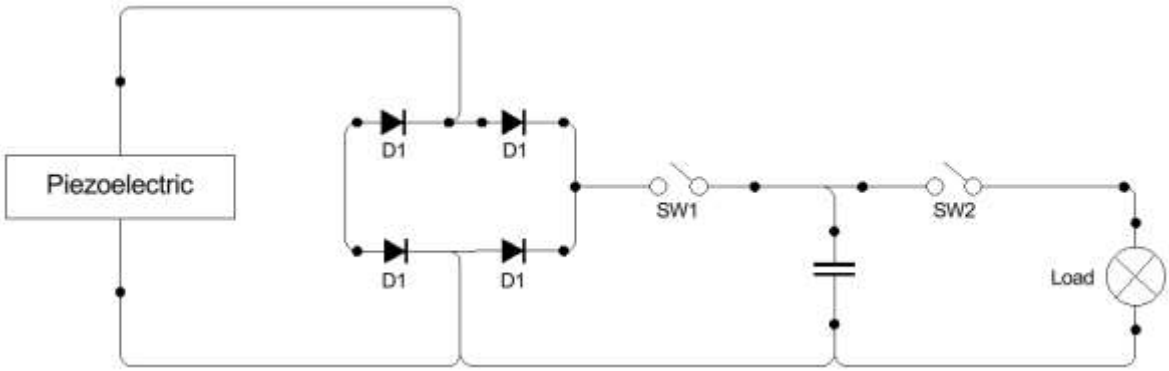

Figure 2. Piezoelectric energy harvesting circuit configuration

Figure 2 illustrates a piezoelectric energy harvesting circuit designed to convert mechanical excitation into measurable electrical energy. The energy source is a piezoelectric cantilever, which generates an alternating (AC) voltage when subjected to mechanical deflection or vibration due to the direct piezoelectric effect. The AC output from the piezoelectric element is connected to a full-wave bridge rectifier composed of four silicon rectifier diodes (D1–D4), type 1N4007. These diodes have a maximum repetitive reverse voltage of 1000 V and a forward current rating of 1 A, with a typical forward voltage drop of approximately 0.7–1.1 V. The 1N4007 diodes are selected due to their high voltage tolerance, availability, and robustness for general-purpose rectification applications. The rectified output is directed to an energy storage stage consisting of a 100 µF electrolytic capacitor, rated at 25 V, with leakage current less than 5 µA. The capacitor functions to accumulate the harvested energy and smooth the pulsating DC signal, thereby reducing ripple and stabilizing the output voltage. Switches SW1 and SW2 are configured as SPST (Single Pole Single Throw) mechanical switches. SW1 controls the connection between the rectifier and the storage capacitor during the charging process, while SW2 isolates or connects the output terminal during measurement. Instead of supplying a resistive load, the output terminal is connected to a DATAQ (DAQ) system for voltage measurement. The DAQ system has a high input impedance (≥1 MΩ) to prevent significant discharge of the storage capacitor

during measurement. The system records the DC voltage across the capacitor over time, enabling analysis of charging characteristics and harvested energy performance.

The experimental setup is illustrated in Figure 3 and consists of a wind-driven piezoelectric energy harvesting system integrated with data acquisition and flow-conditioning components. A wind tunnel (7) is used to generate a controlled and uniform airflow, with a flow straightener (6) installed upstream at a 40° tilt angle to reduce turbulence intensity and ensure stable wind conditions before reaching the test section. A micro windmill (4) is positioned within the airflow and functions as the mechanical excitation source, converting wind energy into rotational motion that induces periodic mechanical interactions with the piezoelectric energy harvester (5). The electrical output generated by the piezoelectric element is routed through a rectifier circuit (3) to convert the alternating voltage into direct current. The rectified signal is then measured and recorded using a DATAQ DI-450 data logger (2), which is connected to a laptop (1) for real-time monitoring, data storage, and post-processing analysis. This configuration enables systematic evaluation of the piezoelectric energy harvester performance under controlled wind-flow conditions and repeatable experimental parameters.

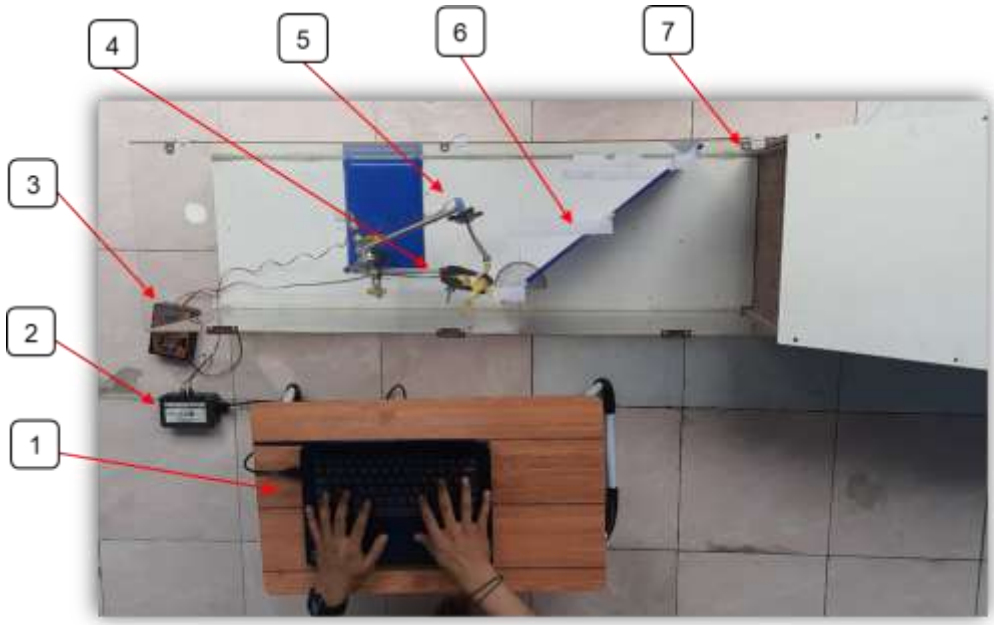

Figure 3. experimental setup

3. RESULTS AND DISCUSSION

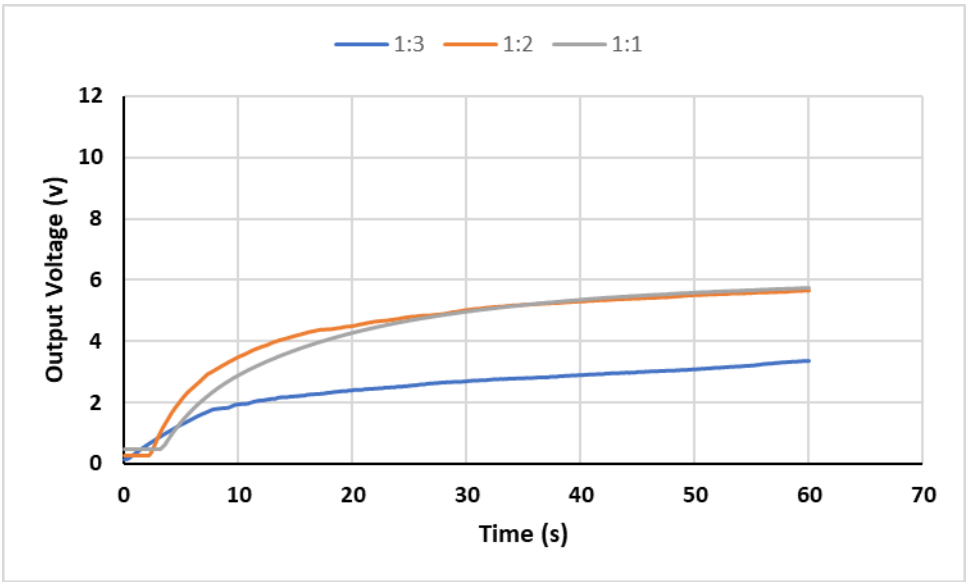

Figure 4. Output Voltage–Time Responses of the System at 6 m/s Wind Speed

e-ISSN: 2830-5418, *p*-ISSN: 2830-5906

At a wind speed of 6 m/s, the output voltage–time responses for the three configuration ratios (1:3, 1:2, and 1:1), as shown in Figure 4, exhibit distinct charging behaviors that reflect differences in energy conversion efficiency. The 1:2 and 1:1 configuration show a rapid initial voltage rise within the first 10–15 s, indicating more effective energy harvesting and rectification under the same airflow conditions. Among these, the 1:2 ratio produces the highest early-stage voltage, suggesting an optimal balance between mechanical excitation and electrical loading that enables faster capacitor charging. After approximately 30 s, both the 1:2 and 1:1 curve begin to converge, reaching a quasi-steady output voltage of about 5.6–5.8 V at 60 s, which implies that the system approaches a saturation condition governed by the circuit and storage capacity rather than wind input alone. In contrast, the 1:3 configuration demonstrates a significantly lower voltage throughout the test duration, with a slower rise and a final voltage of only around 3.3 V at 60 s, indicating reduced energy transfer efficiency, likely due to increased mechanical losses or suboptimal electrical matching. Overall, at a wind speed of 6 m/s, the results indicate that the 1:2 configuration provides the most favorable performance in terms of voltage build-up rate, while the 1:1 configuration yields a comparable steady-state voltage, and the 1:3 configuration is the least effective for energy harvesting under these conditions.

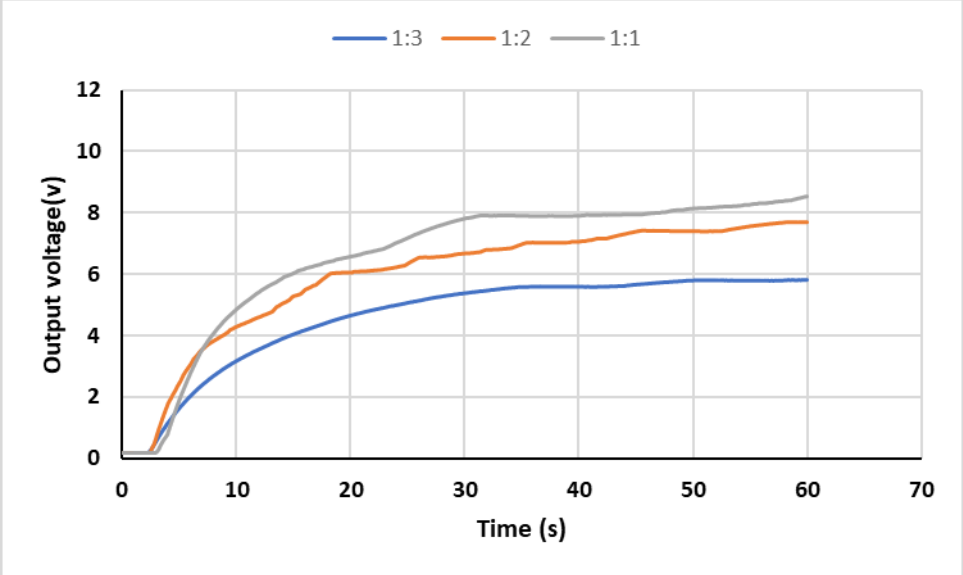

Figure 5. Output Voltage–Time Responses of the System at 7 m/s Wind Speed

At a wind speed of 7 m/s, the output voltage–time characteristics shown in Figure 5 demonstrate an overall improvement in energy harvesting performance compared to lower wind speeds, with clear distinctions among the three configuration ratios (1:3, 1:2, and 1:1). The 1:1 configuration exhibits the fastest voltage rise and the highest output voltage throughout the measurement period, indicating superior mechanical–electrical coupling and more effective energy transfer under increased airflow. The 1:2 configuration also shows a rapid initial increase, reaching a slightly lower but still substantial steady-state voltage, suggesting efficient energy conversion with moderate electrical loading. In contrast, the 1:3 configuration presents a slower voltage build-up and a consistently lower output voltage, although its final voltage is higher than that observed at 6 m/s, reflecting the positive influence of increased wind speed on harvested energy. After approximately 30–40 s, all configurations tend to approach a quasi-steady condition, with final voltages of about 8.4 V, 7.7 V, and 5.8 V for the 1:1, 1:2, and 1:3 ratios, respectively. This convergence behavior indicates that while higher wind speed enhances the charging rate and achievable voltage level, the ultimate output remains constrained by the circuit characteristics and energy storage capacity. Overall, the results at 7 m/s highlight that the 1:1 configuration delivers the most favorable performance in terms of both voltage magnitude and charging speed, followed by the 1:2 configuration, whereas the 1:3 configuration remains the least effective despite benefiting from the increased wind velocity.

At a wind speed of 8 m/s, the output voltage–time responses presented in Figure 6 show a marked enhancement in both charging rate and achievable voltage level for all configuration ratios (1:3, 1:2, and 1:1), confirming the strong influence of increased airflow on the energy harvesting performance. The 1:1 configuration demonstrates the most rapid voltage rise and consistently delivers the highest output voltage throughout the test, reaching a quasi-steady value of approximately 11.4–11.6 V at 60 s. This behavior indicates highly efficient mechanical excitation of the energy harvester and favorable electrical matching that enables

effective energy transfer and storage. The 1:2 configuration exhibits a slightly slower initial rise but still achieves a substantial final voltage of around 9.2 V, reflecting efficient conversion with moderate loading conditions. Meanwhile, the 1:3 configurations show a more gradual voltage increase and attain a lower steady-state voltage of about 8.4 V, suggesting comparatively reduced efficiency due to less optimal coupling between the aerodynamic input and the electrical circuit. After roughly 40–50 s, all curves begin to level off, indicating that the system approaches a saturation condition governed by the capacitor capacity and circuit limitations rather than wind speed alone. Overall, the results in Figure 6 demonstrate that increasing the wind speed to 8 m/s significantly improves energy harvesting performance, with the 1:1 configuration providing the most effective voltage generation, followed by the 1:2 configuration, while the 1:3 configuration remains the least effective despite benefiting from the higher wind velocity.

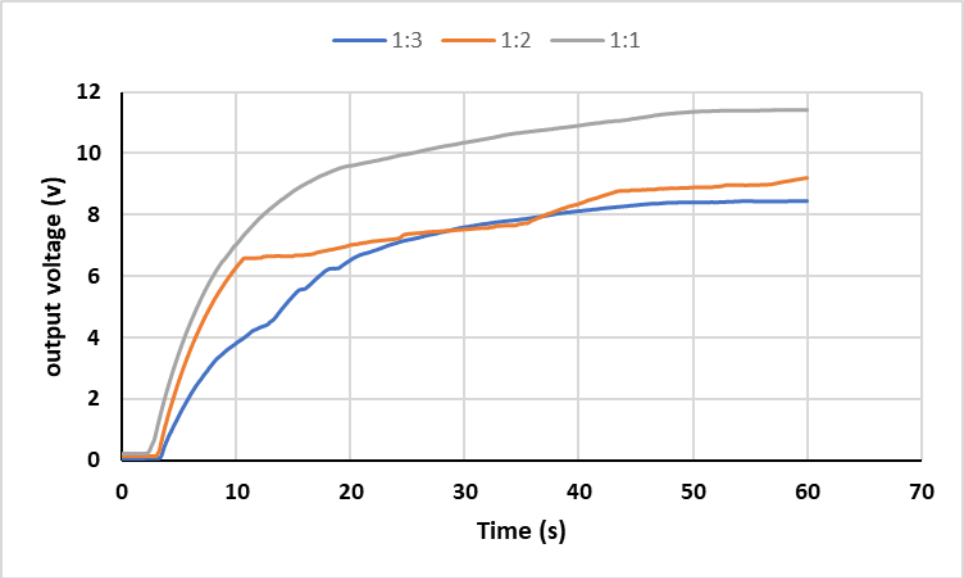

Figure 6. Output Voltage–Time Responses of the System at 8 m/s Wind Speed

A comparison of Figures 4, 5, and 6 reveals a clear and consistent influence of wind speed on the voltage generation and charging behaviour of the energy harvesting system across all configuration ratios (1:3, 1:2, and 1:1). As the wind speed increases from 6 m/s (Figure 4) to 7 m/s (Figure 5) and 8 m/s (Figure 6), both the initial voltage rise and the final steady-state voltage increase significantly, indicating enhanced mechanical excitation and more effective energy conversion. At 6 m/s, the 1:2 and 1:1 configuration exhibit similar steady-state voltages, while the 1:3 configuration remains notably lower. When the wind speed increases to 7 m/s, the performance gap widens, with the 1:1 configuration clearly outperforming the others in both charging rate and final voltage. This trend becomes more pronounced at 8 m/s, where the 1:1 configuration achieves the highest output voltage and fastest charging, followed by the 1:2 configuration, while the 1:3 configuration consistently shows the lowest performance. Across all wind speeds, the curves tend to converge toward a quasi-steady condition after approximately 30–50 s, suggesting that the ultimate voltage is constrained by the electrical circuit and energy storage capacity rather than aerodynamic input alone. Overall, the comparative results demonstrate that increasing wind speed substantially enhances energy harvesting performance and that the 1:1 configuration provides the most favourable and stable output across all tested conditions. These observations align with recent studies suggesting that higher flow velocities intensify the mechanical impact frequency and strain rate, which are critical for overcoming the internal impedance of the rectification circuit [22]. Specifically, the superior performance of the 1:1 ratio supports the principle that optimizes geometric alignment between the excitation source, and the substrate is essential for maximizing energy transfer in collision-based harvesters [23].

4. CONCLUSION

This study has experimentally investigated the performance of a piezoelectric wind energy harvesting system driven by a micro windmill under different wind speeds and substrate-to-blade width ratios. The results demonstrate that wind speed has a significant influence on the output voltage and charging behavior of the system, with higher wind speed leading to faster voltage build-up and higher steady-state voltage levels. Among the tested configurations, the 1:1 ratio consistently produced the highest output voltage and the most stable charging characteristics, particularly at wind speeds of 7 and 8 m/s, indicating more effective mechanical

excitation and energy transfer to the piezoelectric element. The 1:2 configuration showed comparable performance at lower wind speeds, suggesting a favorable balance between excitation frequency and deflection, while the 1:3 configuration exhibited the lowest energy harvesting efficiency across all conditions. Overall, the findings confirm that both mechanical configuration and wind speed are critical parameters in optimizing piezoelectric wind energy harvesters, and the results provide practical guidelines for designing efficient PEH systems for self-powered and low-power electronic applications.

ACKNOWLEDGEMENTS

The authors would like to express their sincere gratitude to all individuals and institutions that contributed to the completion of this research. Special thanks are extended to the Energy Laboratory, as well as the laboratory staff and technicians, for their valuable assistance in setting up the experimental apparatus and operating the wind tunnel facilities.

REFERENCES

[1] H. Jarkov, V., Allan, S. J., Bowen, C., & Khanbareh, "Piezoelectric materials and systems for tissue engineering and implantable energy harvesting devices for biomedical applications," *Int. Mater. Rev.*, vol. 67, no. 7, pp. 683–733, 2021, doi: 10.1080/09506608.2021.1988194.

[2] Z. Zhao, J. Zhu, and W. Chen, "Size-dependent vibrations and waves in piezoelectric nanostructures: a literature review," *Int. J. Smart Nano Mater.*, vol. 13, no. 3, pp. 391–431, Jul. 2022, doi: 10.1080/19475411.2022.2091058.

[3] M. Smith and S. Kar-Narayan, "Piezoelectric polymers: theory, challenges and opportunities," *International Materials Reviews*, vol. 67, no. 1. 2022. doi: 10.1080/09506608.2021.1915935.

[4] C. Tuloup, W. Harizi, Z. Aboura, and Y. Meyer, "Integration of piezoelectric transducers (PZT and PVDF) within polymer-matrix composites for structural health monitoring applications: new success and challenges," *Int. J. Smart Nano Mater.*, vol. 11, no. 4, pp. 343–369, Oct. 2020, doi: 10.1080/19475411.2020.1830196.

[5] J. F. A. Madeira and A. L. Araujo, "Optimal distribution of active piezoelectric elements for noise attenuation in sandwich panels," *Int. J. Smart Nano Mater.*, vol. 11, no. 4, pp. 400–416, Oct. 2020, doi: 10.1080/19475411.2020.1829159.

[6] P. Kurt, B. Narayan, J. I. Roscow, and S. Orhan, "Improving piezoelectric energy harvesting performance through mechanical stiffness matching," *Mech. Adv. Mater. Struct.*, vol. 31, no. 28, pp. 10721–10734, Dec. 2024, doi: 10.1080/15376494.2023.2295383.

[7] H.-Y. Shin, H.-Y. Lee, I.-G. Hong, J.-H. Kim, and J. Im, "Piezoelectric property optimization for piezoelectric single crystals using parametric estimation," *J. Asian Ceram. Soc.*, vol. 11, no. 1, pp. 116–129, Jan. 2023, doi: 10.1080/21870764.2022.2161153.

[8] P. Hajheidari, I. Stiharu, and R. Bhat, "Performance enhancement of cantilever piezoelectric energy harvesters by sizing analysis," *Int. J. Smart Nano Mater.*, vol. 11, no. 2, pp. 93–116, Apr. 2020, doi: 10.1080/19475411.2020.1751743.

[9] D. Cao, W. Qin, Z. Zhou, and W. Du, "Enhancing wind energy harvesting through two V-shaped attachments and monostable characteristics in the galloping piezoelectric harvester," *Energy Convers. Manag.*, vol. 318, p. 118871, Oct. 2024, doi: 10.1016/j.enconman.2024.118871.

[10] C. Xiong *et al.*, "Wave-inspired piezoelectric bistable energy harvester considering stress distribution: Design, simulation and experimental investigation," *Eng. Struct.*, vol. 316, no. July, p. 118535, 2024, doi: 10.1016/j.engstruct.2024.118535.

[11] M. Feri, M. Krommer, and A. Alibeigloo, "Three-dimensional static analysis of a viscoelastic rectangular functionally graded material plate embedded between piezoelectric sensor and actuator layers," *Mech. Based Des. Struct. Mach.*, vol. 51, no. 7, pp. 3843–3867, Jul. 2023, doi: 10.1080/15397734.2021.1943673.

[12] X. Chen *et al.*, "A novel valve-less piezoelectric micropump generating recirculating flow," *Eng. Appl. Comput. Fluid Mech.*, vol. 15, no. 1, pp. 1473–1490, Jan. 2021, doi: 10.1080/19942060.2021.1975573.

[13] Z. Xie and X. Xu, "Experimental study on electro-mechanical response characteristics of PZT5H piezoelectric ceramics under impact loading," *J. Asian Ceram. Soc.*, vol. 9, no. 1, pp. 181–187, Jan. 2021, doi: 10.1080/21870764.2020.1860436.

[14] A. Singh, S. Monga, N. Sharma, K. Sreenivas, and R. S. Katiyar, "Ferroelectric, Piezoelectric Mechanism and Applications," *J. Asian Ceram. Soc.*, vol. 10, no. 2, pp. 275–291, Apr. 2022, doi: 10.1080/21870764.2022.2075618.

[15] A. Supriadi, A. Gamayel, and Y. Z. Arief, "The Influence of Piezoelectric and Fin Material on Piezoelectric-mini wind turbine energy harvester," *J. Glob. Eng. Res. Sci.*, vol. 3, no. 1, pp. 1–6, Jun. 2024, doi: 10.56904/j-gers.v3i1.78.

[16] A. Gamayel and A. Sunardi, "Performance of piezoelectric energy harvester with various ratio substrate and micro windmill," *Telkomnika (Telecommunication Comput. Electron. Control.*, vol. 22, no. 2, pp. 480–487, 2024, doi: 10.12928/TELKOMNIKA.v22i2.25691.

[17] A. Gamayel, M. Zaenudin, and B. W. Dionova, "Performance of piezoelectric energy harvester with vortex-induced vibration and various bluff bodies," *Telkomnika (Telecommunication Comput. Electron. Control.*, vol. 21, no. 4, 2023, doi: 10.12928/TELKOMNIKA.v21i4.24330.

[18] A. Gamayel, "Recent Developments of Piezoelectric Energy Harvester for Scavenging Vibration Energy," *J. Glob. Eng. Res. Sci.*, vol. 3, no. 2, pp. 50–55, Dec. 2024, doi: 10.56904/j-gers.v3i2.110.

[19] M. Khazaee, A. Rezania, and L. Rosendahl, "Piezoelectric resonator design and analysis from stochastic car vibration using an experimentally validated finite element with viscous-structural damping model," *Sustain. Energy Technol. Assessments*, vol. 52, Aug. 2022, doi: 10.1016/j.seta.2022.102228.

[20] Z. Wang, K. Maruyama, and F. Narita, "A novel manufacturing method and structural design of functionally graded piezoelectric composites for energy-harvesting," *Mater. Des.*, vol. 214, Feb. 2022, doi: 10.1016/j.matdes.2021.110371.

[21] M. N. Hasan, M. A. Muktadir, and M. Alam, "Comparative Study of Tapered Shape Bimorph Piezoelectric Energy Harvester via Finite Element Analysis," *Forces Mech.*, vol. 9, Dec. 2022, doi: 10.1016/j.finmec.2022.100131.

[22] Y. Yang, Z. Chen, Q. Kuai, J. Liang, J. Liu, and X. Zeng, "Circuit Techniques for High Efficiency Piezoelectric Energy Harvesting," *Micromachines*, vol. 13, no. 7, p. 1044, Jun. 2022, doi: 10.3390/mi13071044.

[23] J. Wang, M. R. A. Nabawy, A. Cioncolini, A. Revell, and S. Weigert, "Planform Geometry and Excitation Effects of PVDF-Based Vibration Energy Harvesters," *Energies*, vol. 14, no. 1, p. 211, Jan. 2021, doi: 10.3390/en14010211.